Flame Oscillation and Extinction in Buoyancy-suppressed Methane-Air Non-premixed Counter Triple Co-flow Flame

Jin Wook Park[1], Jeong Park[*, 1], Oh Boong Kwon[1], Jin-Han Yun[2], Sang-In Keel[2]

[1]Interdisciplinary Program of Biomedical Engineering, Pukyong National University
[1]Department of Mechanical Engineering, Pukyong National University
[2]Environment & Energy Research Division, Korea Institute of Machinery and Materials

Abstract

Important role of the outermost and inner edge flame was investigated near flame extinction limit in buoyancy-suppressed non-premixed counter-flow flame with triple co-flow burner. The use of He curtain flow produced a microgravity level of 10^{-2}-10^{-3} g in He-diluted non-premixed counter triple co-flow flame experiments. Flame stability map was presented based on flame extinction and oscillation near extinction limit. The stability map via critical diluent mole fraction with global strain rate was represented by varying outer and inner He-diluted mole fractions. Distinct oscillation regimes existed, and the oscillation and extinction modes were quite different each other in terms of the global strain rate and outer and inner He-diluted mole fractions. The flame extinction modes could be classified into five. The result showed that the edge flame was influenced significantly by the conductive heat losses to the flame center or ambient He curtain flow.

Introduction

Since a comprehensive review conducted by Tsuji [1], flame structures and extinction behaviors in a non-premixed counter-flow configuration have been studied extensively [2-6] based on a 1D similarity concept. However, most of these studies focused on highly strained flames, and relatively less concern have been devoted to low-strain-rate flames.

Microgravity experiments with a 14 mm burner diameter showed that low-strain-rate flame extinction can be attributed to radiative heat loss, whereas high-strain-rate flame extinction is caused by flame stretch [7]. Note that a similarity concept is applicable in a counter-flow configuration with an infinite burner diameter and infinite burner gap. The reaction zone thickness was found to be 2~3 cm at a strain-rate of 2 s^{-1} [8]. This implied that the burner diameter should be very large to analyze 1D flame structure and extinction. In this regard, experiments with a skirt-type burner with 230 mm arc length showed that both low- and high-strain-rate flames were extinguished via flame holes which could be a typical form of flame extinction in counter-flow flames [9].

Several studies have focused on low-strain-rate flame extinction that occurs via the shrinkage of the outer edge flame in a counter-flow configuration with finite burner diameters of 18, 26, and 46 mm in normal gravity [10-13]. In reality, the outer-edge region in a non-premixed counter-flow flame has a typical configuration of a partially premixed mixture, such that the edge-flame speed has a functional dependency on the mixture strength, heat losses, local-strain-rate, fuel concentration gradient, and buoyancy. In the previous studies, the outermost partially premixed flame always had a blunt shape, even for low-strain-rate flames [10-13]. This meant that the fuel concentration gradient (and hence the local-strain-rate and inverse of the mixing layer thickness) around the outermost flame edge would be high [14], even for low global-strain-rate flames. Then further extensive studies may be required to understand low strain rate flame extinction and the edge flame behavior in counter-flow configuration.

In the current study, flame extinction and edge flame self-excitations in counter triple co-flow configuration are studied by varying fuel concentrations in the inner and outer fuel nozzle streams and overall strain-rate. Flame stability maps are presented in terms of fuel concentrations in the inner and outer fuel nozzles and overall strain-rate. Particular concerns are focused on self-excitation of the inner and outer edge flames.

Experimental facility

The experimental facility consisted of a counter triple co-flow burner, mass flow controllers, a digital camera system, and a water cooling system as shown in Fig. 1. A counter triple co-flow burner with an inner nozzle diameter (D_{inner}) of 10 mm, an outer nozzle diameter (D_{outer}) of 40 mm, and a curtain flow nozzle diameter ($D_{curtain}$) of 120 mm with a burner gap (L) of 15 mm was used. Air and diluted methane were supplied to the lower and upper nozzles, respectively. The fuel (CH_4), oxidizer (Air), and diluent (He) had purities of 99.95, 99.995, 99.99%, respectively. The flow rates were controlled precisely by using mass flow controllers and a Flow Manager Software (version 3.2). A series of steel fine-mesh screens were positioned to impose plug-flow

* Corresponding author: jeongpark@pknu.ac.kr

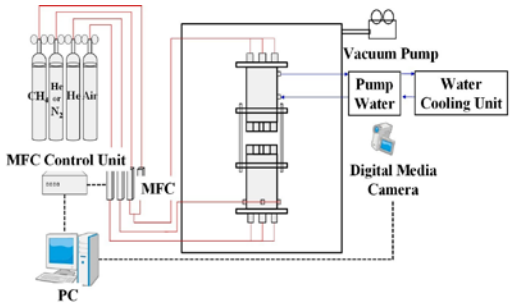

Figure. 1 Schematic of the experimental set-up and flow system in the counter triple co-flow burner.

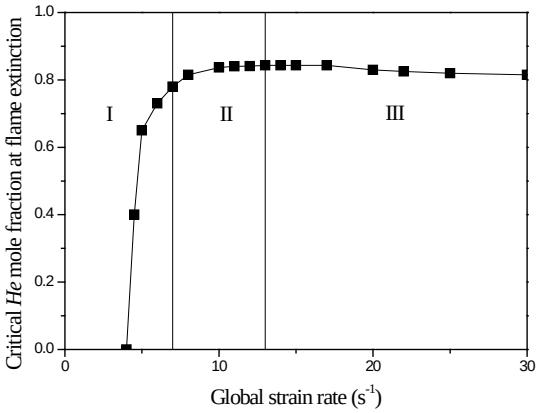

Figure. 2 Critical diluent mole fractions versus global-strain-rate for 40mm burner diameter.

velocity profiles at the burner nozzle exits. A cuboidal compartment was used to avoid external disturbances. Experiments were conducted by varying He diluent mole fraction in the inner and outer nozzle streams for several fixed global-strain-rates.

The global-strain-rate [4] was defined as follows:

$$a_g = \frac{2V_a}{L}\left(1 + V_r \frac{\sqrt{\rho_f}}{\sqrt{\rho_a}}\right),$$

where $V_r = V_f / V_a$ denoted the ratio between the upper and lower nozzle exit velocities. The global-strain-rate was based on the outer fuel nozzle diameter. To evaluate buoyancy effects, density was examined at various flame conditions using the OPPDIF code [15]. At a_g = 10 s^{-1}, the density at the flame zone was 0.165 kg/m^3 for a CH_4-air non-premixed flame, and was in the range of 0.159–0.165 kg/m^3 for He-diluted CH_4-air non-premixed flame. Note that the density of He is 0.164 kg/m^3 at 298 K and 1 atm. Thus the buoyancy force $-(\rho-\rho_\infty)g$ with He curtain flow is estimated to be about 5.0 × 10^{-3} g in He-diluted flames. Therefore, introducing helium curtain flow can suppress buoyancy force in non-premixed counter-flow flame. Based on this idea, helium curtain flow was also adopted in counter triple co-flow burner. The ratio between the upper and lower nozzle exit velocities was always fixed at V_r = 1.0 since, with He curtain flow, the flame was always positioned roughly at the center between the two burners. The He curtain flow velocity was controlled to equal the upper and lower nozzle exit velocities to eliminate shear layer instability.

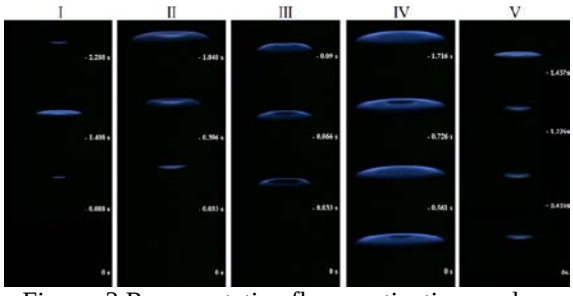

Figure. 3 Representative flame extinction modes.

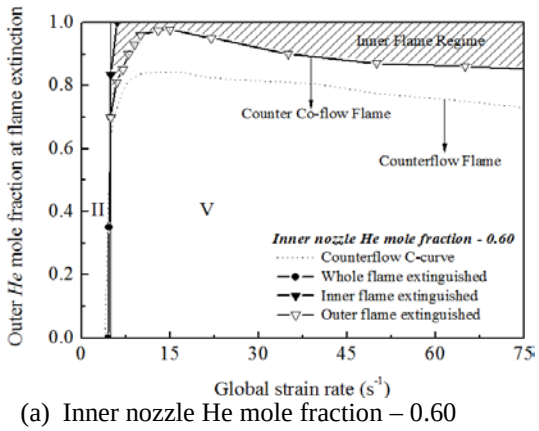

(a) Inner nozzle He mole fraction – 0.60

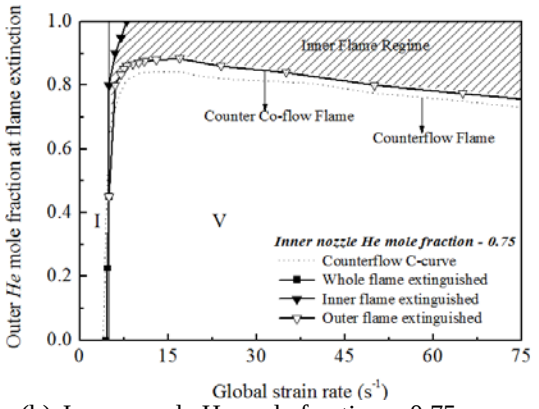

(b) Inner nozzle He mole fraction – 0.75

Figure. 4 He diluent mole fraction in the outer fuel stream versus global-strain-rate.

Results and discussion

Before the research was further proceeded in counter triple co-flow burner, experiments were conducted for the counter-flow burner with only the outer nozzle (40 mm diameter), so that the results could be referred to baseline data. The stability map of counter-flow flame is presented in Fig. 2. The results exhibit a C-curve and three kinds of flame extinction modes similar to the previous researches [10-13] are observed: flame extinction through shrinkage of the outer-edge flame with or without oscillation-of the outer-edge flame prior to the extinction (Regime I or Regime II) and flame extinction through a flame hole at the flame center (Regime III). It is also noted that experiments can be

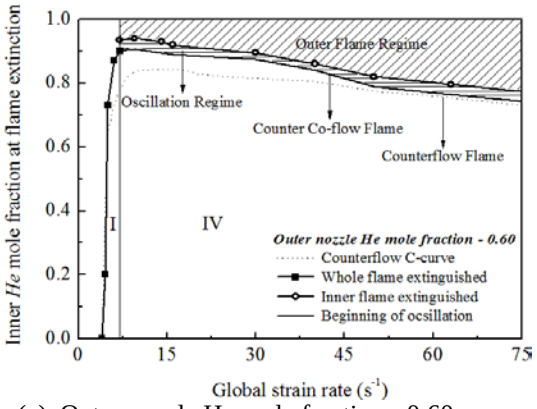

(a) Outer nozzle He mole fraction - 0.60

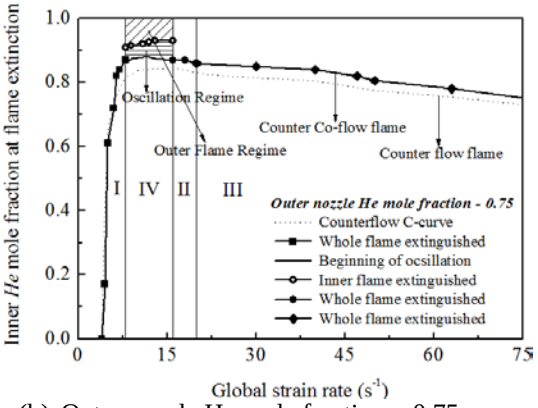

(b) Outer nozzle He mole fraction – 0.75

Figure. 5 He diluent mole fractions in the inner fuel stream versus global-strain-rate.

conducted up to a_g = 4.5 s^{-1} using the present buoyancy-suppressed method. However, at the strain rates less than a_g = 4.5 s^{-1}, the flame could not be sustained due to excessive heat loss from the flame to the ambience of helium curtain flow with a high thermal conductivity.

Based on the baseline data, experiments were also conducted by varying He diluent mole fractions for the inner and outer fuel streams independently in counter triple co-flow burner. Five flame extinction modes were observed as shown in Fig. 3. Regime I denotes a flame extinction via shrinkage of the outermost edge flame after being self-exited, regime II represents a flame extinction via shrinkage of the outermost edge flame without having self-excitation of the outermost edge flame, regime III corresponds to a flame extinction via a flame hole at the flame center without having a self-excitation, regime IV implies self-excitation of both the inner and outermost edge flames followed by either the formation of flame hole at the flame center or extinction of the whole flame, and regime V means either extinction of the whole flame or survival of the inner flame via shrinkage of the outermost edge flame without having self-excitation.

Based on such flame extinction modes, flame stability maps were presented in Fig. 4 and 5 which represents the plot with the fixed He mole fractions (He_{inner}, He_{outer}) in the fuel stream, respectively. The dotted line denotes

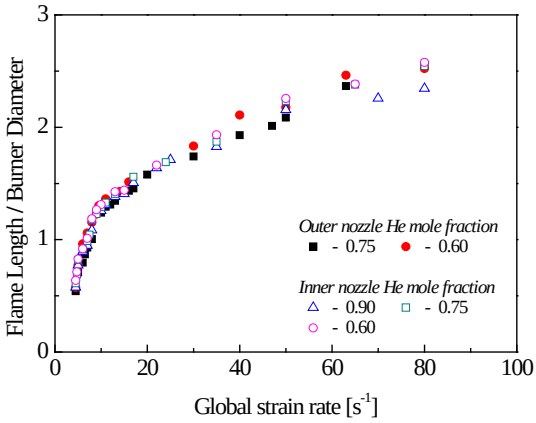

Figure. 6 Normalized Flame Length versus Global-strain-rate.

flame extinction limits of the baseline data, which is the direct outcome from Fig. 2.

In general, counter-flow flames are extinguished via a flame hole at the flame center at high strain rate and are extinguished via shrinkage at low strain rate [10-13]. The He_{inner} is smaller than the flame extinction limits of the baseline data as shown in Fig. 4. In such a situation, flame extinction does not occur through flame hole but through shrinkage of outer nozzle flame (Regime V) at high strain rate. In Fig. 5 (a) the He_{outer} is smaller than flame extinction limits of the baseline data. Contrary to Fig. 4, the flame extinction does not occur through shrinkage of outer nozzle flame but through self-excitation of both the inner and outermost edge flames followed by the formation of flame hole at the flame center (Regime IV). In Fig. 5 (b), regime IV occurs in the same manner as that in Fig. 5 (a). After regime IV, flame extinction limits of the baseline data become smaller. Hence, flame extinction occurs via shrinkage of the outermost edge flame without self-excitation of the outermost edge flame (Regime II). Behind regime II, flame is extinguished via flame hole (Regime III) which is similar to Fig. 2.

Fig. 6 is shown as global-strain-rate with normalized flame length which is related to burner diameter. Flame zone thickness is inversely proportional to strain rate. As shown in Fig. 6, flame length is shorter than burner diameter in low-strain-rate regime (a_g < 7 s^{-1}). Furthermore, in stability maps (Fig. 4, Fig. 5), regime1 is shown as low strain rate regime which means that with a finite burner diameter and a finite burner gap, it becomes hard to analyze in 1D similarity concept. Subsequently, in low-strain-rate regime, apart from radiative heat loss, the widely known dominative factor in low-strain-rate flame extinction, other predominating factors may also exist. Hence, it is necessary to concern conductive heat loss in 2D radial direction in counter triple co-flow burner. For more in-depth study of flame extinction and edge flame behavior in counter flow configuration, further research is being conducted through experiments and numerical simulations.

Conclusions

Flame extinction and edge flame self-excitations in counter triple co-flow configuration have been studied by varying fuel concentrations in the inner and outer fuel nozzle streams and overall strain-rate. The following conclusion can be drawn:

1) For a 40 mm counter-flow burner to achieve baseline data, three kinds of flame extinction modes was attained, and the curve of critical diluent mole fraction versus global strain rate was of C-shape. Applying the buoyancy-suppressed experimental method (adopting He-curtain flow) could extend the experiments up to $a_g = 4.5\ s^{-1}$.

2) The flame extinction modes of Triple Co-flow burner are classified into five modes:

(I) an extinction through the shrinkage of the outmost edge flame forward to the flame center after self-excitation,

(II) an extinction through the shrinkage of the outmost edge flame forward to the flame center without self-excitation,

(III) an extinction through rapid advancement of a flame hole while the outmost edge flame is stationary,

(IV) occurrence of self-excitation in the outermost edge flame and the center edge flame followed by either the formation of donut shaped flame or the extinction of the entire flame,

and (V) shrinkage of the outermost edge flame without self-excitation followed by shrinkage or survival of the center flame.

3) Flame stability maps are presented in terms of fuel concentration in the inner and outer fuel nozzles and overall strain-rates. When the He_{inner} is smaller than the flame extinction limits of the baseline data, flame extinction does not occur through flame hole but through shrinkage of outer nozzle flame (Regime V) at high strain rate. Contrarily, when the He_{outer} is smaller than flame extinction limits of the baseline data, the flame extinction does not occur through shrinkage of outer nozzle flame but through self-excitation of both the inner and outermost edge flames followed by the formation of flame hole at the flame center (Regime IV).

4) Apart from radiative heat loss other predominating factors may also exist in low-strain-rate regime. It is necessary to concern conductive heat loss in 2D radial direction in counter triple co-flow burner.

Acknowledgement

This research was supported by the Space Core Technology Development Program through the National Research Foundation of Korea (NRF) funded by the Ministry of Education, Science, and Technology.

References

[1] H. Tsuji, Prog Energy Combust Sci 9 (1982) 93-119.

[2] M.D. Smooke, I. K. Puri, K. Seshadri, Proc Combust Inst 21 (1986) 1783-1792.

[3] N. Peters, R. J. Kee, Combust Flame 68 (1987) 17-29.

[4] H. K. Chelliah, C. K. Law, T. Ueda, M. D. Smooke, F. A. Williams, Proc Combust Inst 23 (1998) 503-511.

[5] C. -J. Sung, J. B. Liu, C. K. Law, Combust Flame 102 (1995) 481-492.

[6] M. D. Smooke, R. A. Yetter, T. P. Parr, D. M. Hanson-Parr, M. A. Tanoff, M. B. Colket, R. J. Hall, Proc Combust Inst 28 (2000) 2013-2020.

[7] Maruta K, Yoshida M, Guo H, Ju Y, Niioka T, Combust Flame 112 (1997) 181-187.

[8] F. C. Frate, H. Bedir, C. J. Sung, J. S. Tien, Proc Combust Inst 28 (2000) 2047-2054.

[9] Han B, Ibarreta AF, Sung CJ, Tien JS, Proc Combust Inst 30 (2005) 527-535.

[10] D. G. Park, J. H. Yun, J. Park, S. I. Keel, Energy & Fuels 23 (2009) 4236-4244.

[11] J. S. Park, D. J. Hwang, J. Park, J. S. Kim, S. C. Kim, S. I. Keel, T. K. Kim, D. S. Noh, Combust. Flame 146 (2006) 612-619.

[12] C. B. Oh, Hamins A, Bundy M, J. Park, Combust. Theory Modeling 12 (2008) 283-302.

[13] Y. H. Chung, D. G. Park, J. H. Yun, J. Park, O. B. Kwon, S. I. Keel, Fuel, 105 (2013) 540-550.

[14] S. H. Chung, Proc. Combust. Inst., 31 (2007) 877–892.

[15] A.E. Lutz, R.J. Kee, J. F. Grcar, G.A. Dixon-Lweis, SAND96-8243, Sandia Natl Laboratories Rep 1997.